

Experimentally observable signatures of odd-frequency pairing in multiband superconductorsL. Komendová,¹ A. V. Balatsky,^{2,3} and A. M. Black-Schaffer^{1,*}¹*Department of Physics and Astronomy, Uppsala University, Box 530, SE-751 21 Uppsala*²*NORDITA, Center for Quantum Materials, KTH Royal Institute of Technology, and Stockholm University, Roslagstullsbacken 23, SE-106 91 Stockholm, Sweden*³*Institute for Materials Science, Los Alamos National Laboratory, Los Alamos, New Mexico 87545, United States*

(Received 17 June 2015; revised manuscript received 10 August 2015; published 30 September 2015)

We investigate how hybridization (single-quasiparticle scattering) between two superconducting bands induces odd-frequency superconductivity in a multiband superconductor. An explicit derivation of the odd-frequency pairing correlation and its full frequency dependence is given. We also find that the density of states is modified, at higher energies, from the sum of the two BCS spectra to also include additional hybridization gaps with strong coherence peaks when odd-frequency pairing is present. These gaps constitute clear experimentally measurable signatures of odd-frequency pairing in multiband superconductors.

DOI: [10.1103/PhysRevB.92.094517](https://doi.org/10.1103/PhysRevB.92.094517)

PACS number(s): 74.45.+c, 74.20.Mn, 74.20.Rp, 74.50.+r

I. INTRODUCTION

Many materials have multiple bands close to the Fermi level. It is then not surprising that there also exist many superconductors with more than one superconducting band. Well-known multiband superconductors are MgB_2 [1–3], which hosts two distinct superconducting gaps, and the iron-based superconductors [4–6], where the order parameter even changes sign between different bands [7,8]. Multiband superconductivity has also been suggested to be important in simple metals [9,10], heavy fermion compounds [11–15], different carbides [16,17], and Chevrel phases [18], as well as for engineering time-reversal invariant topological superconducting states [19,20].

Multiple superconducting bands allow for unusual coupling effects. Early, and much current, theoretical focus has been oriented towards studying the effects of Josephson coupling between different superconducting bands, i.e., the exchange of whole Cooper pairs between bands [21–26]. However, single-quasiparticle scattering, or tunneling, between the superconducting bands is conceptually much simpler. The origin of interband quasiparticle scattering can be impurity scattering, but a common intrinsic source is the superconductivity associated with specific orbitals, which subsequently hybridize to form the low-energy bands around the Fermi surface. Tunneling spectroscopy has found significant effects of interband quasiparticle scattering in silicon clathrate $\text{Ba}_8\text{Si}_{46}$ [27,28], iron-based superconductors [29], and MgB_2 [30]. Recent ARPES data on MgB_2 have also shown that interband scattering due to disorder can be important [31].

Theoretically, interband single-quasiparticle scattering results in both band hybridization and *interband* pairing, where the two electrons forming a Cooper pair belong to *different* bands. Straightforward effects of band hybridization were studied already quite early on [32–34]. More recently, band hybridization has also been proposed to influence the nodal structure of the superconducting gap in iron-based superconductors [35–38]. On the other hand, consequences of the

induced interband pairing have been much less discussed. Pure interband pairing in cold atom and quantum chromodynamics systems has been proposed to give a “breached” regime containing both a superfluid and a normal liquid [39,40], but in band-hybridized superconductors the interband pairing is also accompanied by (usually large) conventional intraband pairings. Still, it was recently pointed out, using symmetry arguments and simple mean-field BCS calculations, that superconducting pairing which is odd in both frequency and band index can be ubiquitous in multiband superconductors, although the explicit frequency dependence was never found [41].

The fermionic nature of the superconducting wave function usually renders a division into spin-singlet even-parity (i.e., *s*-, *d*-wave) or spin-triplet odd-parity (*p*-wave) superconductors, but it can also be even or odd under time, or equivalently frequency [42–44]. Examples of this are odd-frequency spin-triplet *s*-wave superconductivity giving rise to long-range proximity effects in superconductor-ferromagnet systems [45,46] or odd-frequency spin-singlet *p*-wave pairing in nonmagnetic junctions [47–49]. A recent example of the former is the theoretically predicted odd-frequency pairing in MgB_2 under applied magnetic field [50]. In multiband superconductors, the band index offers the additional possibility of spin-singlet *s*-wave pairing, which is odd in both band and frequency, without translation or spin rotation symmetry breaking or any external fields.

In this work, we derive the exact Green’s functions for a generic multiband superconductor with single-quasiparticle scattering. We thus obtain the full frequency dependence of the interband pairing and find that the odd-interband pairing has odd-frequency dependence, while the even-interband pairing is even in frequency. By studying the density of states (DOS), we also discover that finite band hybridization gives rise to an extra gap located beyond the original gap edges. This hybridization-induced gap is not fully depleted, but still has very pronounced BCS-like coherence peaks. Moreover, the hybridization gap disappears whenever the odd-frequency interband pairing is absent and is thus a directly measurable signal of odd-frequency superconductivity.

*annica.black-schaffer@physics.uu.se

II. RESULTS

To model a generic multiband superconductor, we consider two bands, bands 1 and 2, with dispersions ϵ_{k1} and ϵ_{k2} , where $\epsilon_k = \epsilon_{-k}$. For simplicity, we assume that the two bands independently develop conventional spin-singlet s -wave superconducting order parameters Δ_1 and Δ_2 , respectively, but one of them can also be zero. Finally, we add a small single-quasiparticle hybridization, or scattering, term proportional to Γ between the two bands, resulting in the Hamiltonian

$$H = \sum_{k\sigma} \epsilon_{k1} a_{k\sigma}^\dagger a_{k\sigma} + \epsilon_{k2} b_{k\sigma}^\dagger b_{k\sigma} + \sum_{k\sigma} \Gamma(k) a_{k\sigma}^\dagger b_{k\sigma} + \text{H.c.} \\ + \sum_k \Delta_1(k) a_{k\uparrow}^\dagger a_{-k\downarrow}^\dagger + \Delta_2(k) b_{k\uparrow}^\dagger b_{-k\downarrow}^\dagger + \text{H.c.}, \quad (1)$$

where a (b) is the annihilation operator in band 1 (2). Alternatively, the band hybridization can be interpreted as a coupling process in real space, with the a and b electrons living to the left and the right of a junction or in different layers [32,51]. In this picture, the Josephson coupling would instead be a two-particle tunneling term (not included here).

We start by calculating the spin-singlet s -wave interband anomalous Green's functions F_{12} and F_{21} , which express the pairing correlations of two electrons belonging to different bands. Assuming Γ to be a small parameter, we can use standard perturbation theory [52]. The first-order contributions are then represented by the schematic diagrams in the inset of Fig. 1(a) and give $F_{12}^{(1)} = F_1 \Gamma G_2 - \overleftarrow{G}_1 \Gamma F_2$, where \overleftarrow{G} is

the hole propagator, i.e., $\overleftarrow{G} = -G(-k, -\omega)$. The minus sign before the second term is due to scattering of hole propagators (left-going arrows). The normal and anomalous propagators without the hybridization are as usual [52]

$$\begin{pmatrix} G_j & F_j \\ F_j^\dagger & \overleftarrow{G}_j \end{pmatrix} = \frac{1}{(i\omega)^2 - E_j^2} \begin{pmatrix} i\omega + \epsilon_{kj} & \Delta_j \\ \Delta_j^* & i\omega - \epsilon_{kj} \end{pmatrix}, \quad (2)$$

where $E_j^2 = E_{kj}^2 = \epsilon_{kj}^2 + |\Delta_j|^2$ and $\omega = \omega_n = \pi(2n+1)k_B T$ are the fermionic Matsubara frequencies. Using these expressions we arrive at $F_{12}^{(1)} = \Gamma[i\omega(\Delta_1 - \Delta_2) + \Delta_1\epsilon_{k2} + \Delta_2\epsilon_{k1}]/[(\omega^2 + E_1^2)(\omega^2 + E_2^2)]$. The next-to-leading-order terms for F_{12} are cubic in Γ . Further organizing the perturbation expansion of the interband pairing of a given order n in a systematic way, we find several recursion relationships (see Appendix for a detailed derivation). These can be compactly written in a matrix form as

$$\begin{pmatrix} \overleftarrow{G}_{12}^{(n)} \\ F_{12}^{(n)} \end{pmatrix} = g \begin{pmatrix} e & f \\ -f^* & e^* \end{pmatrix} \begin{pmatrix} \overleftarrow{G}_{12}^{(n-2)} \\ F_{12}^{(n-2)} \end{pmatrix}, \quad (3)$$

where $g = \Gamma^2/[(\omega^2 + E_{k1}^2)(\omega^2 + E_{k2}^2)]$, $e = (i\omega - \epsilon_{k1})(i\omega - \epsilon_{k2}) - \Delta_1\Delta_2^*$, and $f = -i\omega(\Delta_1^* - \Delta_2^*) + \Delta_1^*\epsilon_{k2} + \Delta_2^*\epsilon_{k1}$. For the starting point of the recursion, we use the first-order anomalous interband Green's function $F_{12}^{(1)}$ and the corresponding normal propagator: $\overleftarrow{G}_{12}^{(1)} = \Gamma[\Delta_1\Delta_2^* - (i\omega - \epsilon_{k1})(i\omega - \epsilon_{k2})]/[(\omega^2 + E_1^2)(\omega^2 + E_2^2)]$. From Eq. (3), we recognize that the Green's functions to infinite order can be written as a geometric series, where the quotient is a two-by-two matrix. The formal criterion for a matrix geometric series to be convergent is that the norm (i.e., the largest singular value) of the coefficient matrix is < 1 . From this, we arrive at the condition $\Gamma \lesssim (\omega^2 + E_1^2)^{1/4}(\omega^2 + E_2^2)^{1/4}$, which translates into

$$\Gamma \lesssim \sqrt{|\Delta_1||\Delta_2|}, \quad (4)$$

meaning that the series is always convergent for sufficiently small Γ , provided that Δ_1 and Δ_2 are both finite. This allows us to sum the infinite series and we arrive at $F_{12} = \Gamma[i\omega(\Delta_1 - \Delta_2) + \Delta_2\epsilon_{k1} + \Delta_1\epsilon_{k2}]/D$, where $D = (\omega^2 + E_1^2)(\omega^2 + E_2^2) - \Gamma^2[2(\epsilon_{k1}\epsilon_{k2} - \omega^2) - \Delta_2^*\Delta_1 - \Delta_1^*\Delta_2] + \Gamma^4$. The expression for F_{21} is obtained by exchanging the band indices and we can also form the odd and even combinations of F_{12} and F_{21} with respect to the band index:

$$F_{12}^{\text{odd}}(\mathbf{k}, i\omega) = \frac{F_{12} - F_{21}}{2} = i\omega\Gamma(\Delta_1 - \Delta_2)/D, \quad (5)$$

$$F_{12}^{\text{even}}(\mathbf{k}, i\omega) = \frac{F_{12} + F_{21}}{2} = \Gamma(\Delta_1\epsilon_{k2} + \Delta_2\epsilon_{k1})/D. \quad (6)$$

The odd-band combination is directly seen to be odd in frequency, whereas the even-band combination has a conventional even-frequency dependence. This is fully consistent with Fermi-Dirac statistics for spin-singlet s -wave superconducting pairing. Furthermore, we see that interband pairing always requires a finite band hybridization and that the odd-interband pairing also requires $\Delta_1 \neq \Delta_2$. Equations (5) and (6) can be Fourier transformed to real space and then evaluated numerically, with the result shown in Fig. 1. By definition,

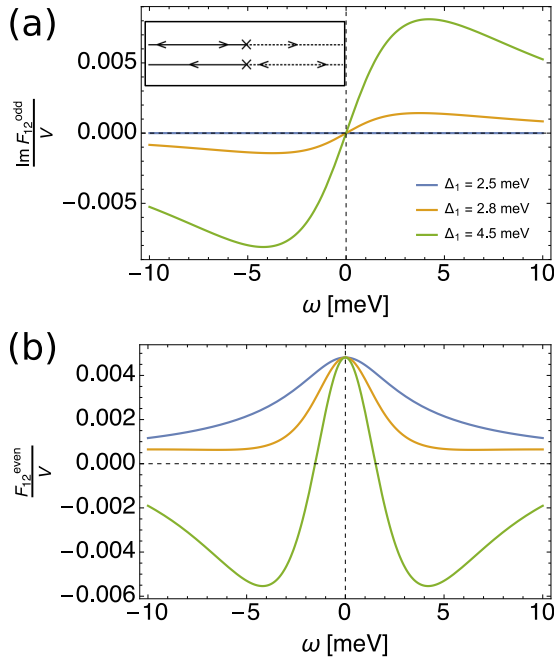


FIG. 1. (Color online) (a) Odd- and (b) even-interband pairing amplitudes in meV per nm³ when $\Delta_2 = 2.5$ meV, $\Delta_1 = 2.5, 2.8, 4.5$ meV (blue, orange, green), and $\Gamma = 3$ meV, with the band structure specified in the main text. (Inset:) First-order hybridization contributions to the interband pairing: $F_1 \Gamma G_2$ (top) and $-\overleftarrow{G}_1 \Gamma F_2$ (bottom). Solid (dashed) line represents the propagator in band 1 (2) and \times the hybridization.

the odd-frequency pairing amplitude must be zero at $\omega = 0$. Close to $\omega = 0$, we find that the leading term in F^{odd} is linear in ω . However, the slope can initially be large and then abruptly change sign to asymptotically go to zero for large ω , resulting in an approximate $1/\omega$ -dependence, which has also been found for some odd-frequency states [53,54].

By forming an analog of Eq. (3) for the intraband anomalous Green's function in band 1, we find $F_1 = \{\Delta_1[(i\omega)^2 - E_2^2] - \Gamma^2\Delta_2\}/D$ and the corresponding normal Green's function: $G_1 = \{(i\omega + \epsilon_{k1})[(i\omega)^2 - E_2^2] - \Gamma^2(i\omega - \epsilon_{k2})\}/D$. The expressions for F_2 and G_2 are obtained by mutually exchanging band indices. The expressions for the normal Green's functions allow us to compute the DOS using the standard formula:

$$N(E) = -\frac{1}{\pi} \text{Im Tr } G(E + i\delta), \quad \delta \rightarrow 0^+. \quad (7)$$

Here the trace involves a sum over band and spin indices and an integral over k space. We use similar expressions, but unsummed over the band index, to define the partial DOS N_1 and N_2 .

The total and partial DOS offer a direct connection to experimental measurements on multiband superconductors. In Figs. 2–4, we show numerically obtained results for the DOS, explicitly exploring the effect of interband pairing. To most clearly illustrate the effect of interband pairing, we use two generic parabolic bands: $\epsilon_{kj} = \hbar^2 k^2/2m_j - \mu_j$, with effective masses $m_1 = 20m_e$, $m_2 = 22m_e$, and distances from the bottom of the bands to the Fermi level $\mu_1 = 100$ meV and $\mu_2 = 105$ meV. For this and other band structures, we studied, the interband effects are most clearly visible when Γ is comparable to $|\epsilon_{k1} - \epsilon_{k2}|$ for fixed $k \approx k_F$. The contributions to the DOS are obtained by numerical integration in the range including both Fermi surfaces and we use a smearing parameter $\delta = 0.01$ meV. We have also independently verified the DOS results by direct numerical diagonalization of the Hamiltonian in Eq. (1). In fact, we find a perfect agreement even far beyond the theoretical condition for convergence in Eq. (4).

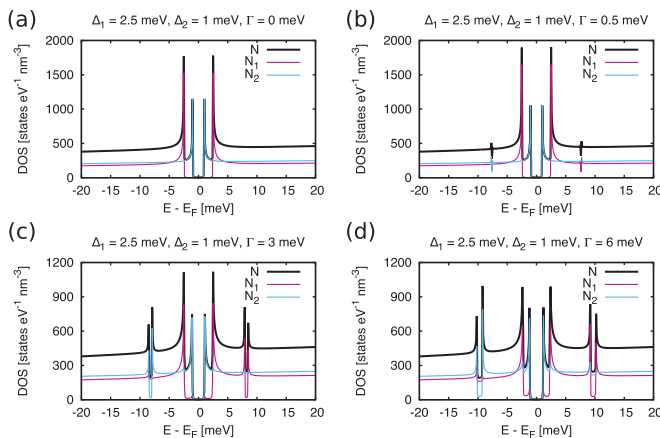


FIG. 2. (Color online) Total (N) and partial densities of states (N_1, N_2) when $\Delta_1 = 2.5$ meV and $\Delta_2 = 1$ meV for different values of $\Gamma = 0, 0.5, 3, 6$ meV [(a)–(d)], with the band structure specified in the main text.

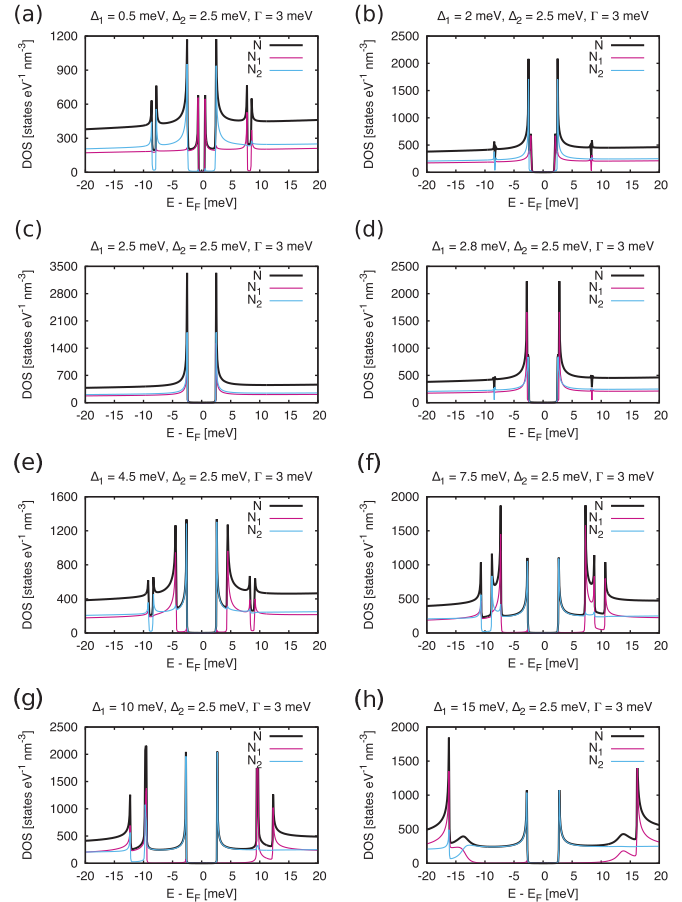


FIG. 3. (Color online) Total (N) and partial densities of states (N_1, N_2) when $\Delta_2 = 2.5$ meV and $\Gamma = 3$ meV for different values of $\Delta_1 = 0.5, 2, 2.5, 2.8, 4.5, 7.5, 10, 15$ meV [(a)–(h)], with the band structure specified in the main text.

We here especially showcase that unusual features in the DOS are only seen when the conditions $\Gamma \neq 0$ and $\Delta_1 \neq \Delta_2$ are both satisfied, which are exactly the two key criteria for odd-frequency pairing, see Eq. (5). First, the DOS without any band hybridization, as shown in Fig. 2(a), is just a sum of two BCS spectra with energy gaps $E_{g1} = \Delta_1$ and $E_{g2} = \Delta_2$, respectively, as expected. However, when we turn on hybridization, see Figs. 2(b)–2(d), we see extra, very notable, dips in the DOS located beyond the original gap edges $E_{g1,2}$. These dips, symmetrically located around zero energy, clearly resemble superconducting gaps with their pronounced BCS-like coherence peaks. However, the DOS in the gap regions are not zero, but instead equal to the partial DOS at these energies. Still, we here refer to these features as hybridization-induced gaps. The hybridization-induced gaps grow in size and move to higher energies for larger band hybridizations, and we thus associate these features with interband superconducting pairing. Their position in energy can be explained from the numerically obtained spectrum of Hamiltonian (1), shown in Fig. 5. Panel (a) shows the hybridized bands close to the Fermi energy in the normal state, while in panel (b), the two bands are superconducting and two full gaps thus exist at the Fermi energy. However, at the position where the electron band ϵ_{k1} crosses the hole band $-\epsilon_{k2}$

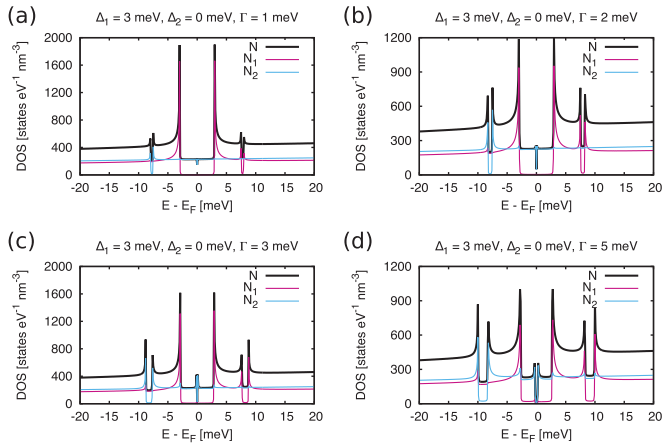


FIG. 4. (Color online) Total (N) and partial densities of states (N_1 , N_2) when $\Delta_1 = 3 \text{ meV}$ and $\Delta_2 = 0$, i.e., only one band with native superconductivity, for different values of $\Gamma = 1, 2, 3, 5 \text{ meV}$ [(a)–(d)] with the band structure specified in the main text.

(and opposite, i.e., ϵ_{k2} crosses $-\epsilon_{k1}$), hybridization-induced interband gaps also open in the superconducting state. Since the superconducting gaps $\Delta_{1,2}$ are generally the smallest energy scale, the hybridization-induced gaps will be located beyond the BCS gaps $E_{g1,2}$. Thus the position of the hybridization-induced gaps is determined by the normal state band structure, but they only appear when superconductivity is present. This phenomenon is similar to what has very recently been observed in nanoscale superconductors [55]. The reason for multiple bands and interband pairing in that case is the spatial confinement and the spatially dependent gap amplitude $\Delta(\vec{r})$. We note that beyond the hybridization-induced gaps, we see no other distinctive features associated with interband pairing. Notably, there are no zero-energy or subgap states, otherwise often associated with odd-frequency pairing [43,48,49,56–59]. Recent works have pointed out that zero-energy states do not always accompany odd-frequency pairing [41,54,60,61], and odd-frequency, odd-interband pairing studied here provides another example when this happens.

In Fig. 3, we instead fix $\Gamma = 3 \text{ meV}$, and $\Delta_2 = 2.5 \text{ meV}$ but vary Δ_1 . Distinct hybridization-induced gaps are again present at energies beyond the original gap edges, independent on the relative size of the two original gaps. The only exception is exactly when $\Delta_1 = \Delta_2$, then the hybridization-induced gaps completely disappear, despite the finite band hybridization, see Fig. 3(c). Detuning the value of Δ_1 slightly from that of Δ_2 results in small, but noticeable, dips in the DOS, at the positions where the full gaps develop for increasing differences between Δ_1 and Δ_2 . We thus find that the hybridization-induced gaps are only present in the DOS when both $\Gamma \neq 0$ and $\Delta_1 \neq \Delta_2$. These are exactly the two key criteria for odd-frequency pairing, as seen in Eq. (5). In fact, only the odd-frequency interband pairing disappears at $\Delta_1 = \Delta_2$, the even-frequency part is in general nonzero as soon as $\Gamma \neq 0$. Specifically, the even- and odd-frequency interband pairing amplitudes corresponding to the parameters in Figs. 3(c)–3(e) are plotted in Fig. 1. From there it is clear that the even-frequency interband pairing is large and not changing significantly around $\omega = 0$, while the odd-frequency

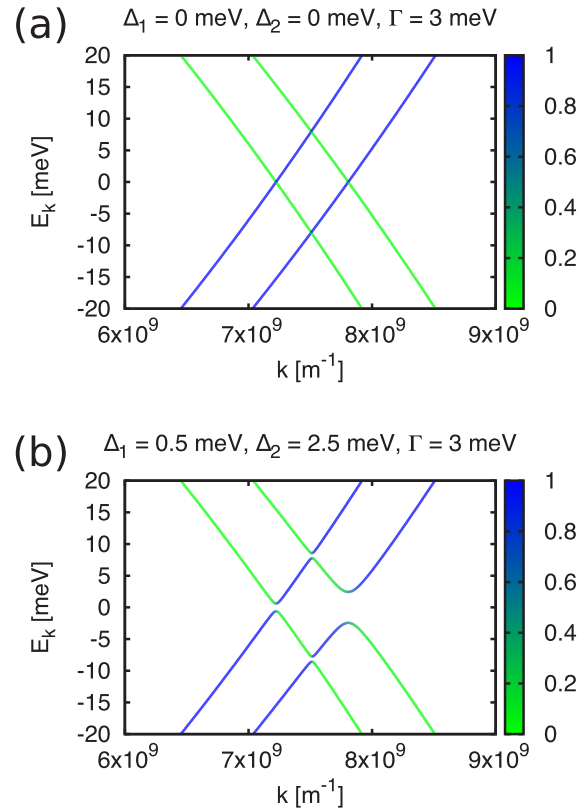


FIG. 5. (Color online) Hybridized bands in the normal state (a) (bands are doubled due to particle-hole symmetry in the Hamiltonian) and in the superconducting state (b). Green (light) color corresponds to hole character, blue (dark) to electron character. The band structure is specified in the main text and the density of states for (b) is shown in Fig. 3(a).

part changes from identically zero in Fig. 3(c) to a notable nonzero derivative at $\omega = 0$ for Figs. 3(d) and 3(e). We can thus conclude that odd-frequency interband pairing is necessary for producing the hybridization-induced gaps. Detecting gaps beyond the original two superconducting gaps in multiband superconductors is therefore a clear sign of the presence of odd-frequency pairing. Intriguingly, additional gap features have already been reported in the multiband superconductor $\text{Ba}_8\text{Si}_{46}$ [27].

Finally, we also show that only one band has to be natively superconducting for the hybridization-induced gaps to be present. In Fig. 4, we display how the hybridization-induced gap grows with increasing Γ when $\Delta_2 = 0$. A finite single-particle hybridization Γ results in a proximity-induced gap also in the second band, which is manifested as a gap around zero energy, although always smaller than $E_{g1} = \Delta_1$. For all parameter choices in Fig. 4, the spectrum always has a gap at zero energy, i.e., there are no zero-energy states. This is not clearly seen in Fig. 4(a) due to the finite smearing parameter, but it is clearly visible in the numerical diagonalization results which do not suffer from the same problem. In addition, a finite Γ results in finite odd-frequency interband pairing, and we consequently also see hybridization-induced gaps beyond the Δ_1 gap, which also grow with Γ . In fact, these gaps are much more pronounced than the proximity-induced gap in band 2 at zero energy.

where $g = \Gamma^2/[(\omega^2 + E_{k_1}^2)(\omega^2 + E_{k_2}^2)]$, $e = (i\omega - \epsilon_{k_1})(i\omega - \epsilon_{k_2}) - \Delta_1\Delta_2^*$, and $f = -i\omega(\Delta_1^* - \Delta_2^*) + \Delta_1^*\epsilon_{k_2} + \Delta_2^*\epsilon_{k_1}$.

This is a matrix geometric series and is thus easily summed giving

$$\begin{pmatrix} \overleftarrow{G}_{12} \\ F_{12} \end{pmatrix} = q \begin{pmatrix} 1 - ge^* & gf \\ -gf^* & 1 - ge \end{pmatrix} \begin{pmatrix} \overleftarrow{G}_{12}^{(1)} \\ F_{12}^{(1)} \end{pmatrix}, \quad (\text{A9})$$

where $q = [(1 - ge)(1 - ge^*) + g^2|f|^2]^{-1}$ and $\overleftarrow{G}_{12}^{(1)} = \overleftarrow{\langle \dots \rangle} = \Gamma[\Delta_1\Delta_2^* - (i\omega - \epsilon_{k_1})(i\omega - \epsilon_{k_2})]/[(\omega^2 + E_{k_1}^2)(\omega^2 + E_{k_2}^2)]$. Some terms cancel and we get $F_{12} = qF_{12}^{(1)}$. Finally, $F_{12} = \Gamma[i\omega(\Delta_1 - \Delta_2) + \Delta_2\epsilon_{k_1} + \Delta_1\epsilon_{k_2}]/D$, where $D = (\omega^2 + E_1^2)(\omega^2 + E_2^2) - \Gamma^2[2(\epsilon_{k_1}\epsilon_{k_2} - \omega^2) - \Delta_2^*\Delta_1 - \Delta_1^*\Delta_2] + \Gamma^4$. For the normal propagator G_1 , needed for calculating the DOS, we create a matrix equation together with F_1^\dagger , otherwise the procedure proceeds in the same manner as above.

-
- [1] J. Nagamatsu, N. Nakagawa, T. Muranaka, Y. Zenitani, and J. Akimitsu, Superconductivity at 39 K in magnesium diboride, *Nature (London)* **410**, 63 (2001).
- [2] H. J. Choi, D. Roundy, H. Sun, M. L. Cohen, and S. G. Louie, The origin of the anomalous superconducting properties of MgB₂, *Nature (London)* **418**, 758 (2002).
- [3] S. Souma, Y. Machida, T. Sato, T. Takahashi, H. Matsui, S.-C. Wang, H. Ding, A. Kaminski, J. C. Campuzano, S. Sasaki, and K. Kadowaki, The origin of multiple superconducting gaps in MgB₂, *Nature (London)* **423**, 65 (2003).
- [4] Y. Kamihara, T. Watanabe, M. Hirano, and H. Hosono, Iron-Based Layered Superconductor La[O_{1-x}F_x]FeAs ($x = 0.05-0.12$ with $T_c = 26$ K), *J. Am. Chem. Soc.* **130**, 3296 (2008).
- [5] F. Hunte, J. Jaroszynski, A. Gurevich, D. C. Larbalestier, R. Jin, A. S. Sefat, M. A. McGuire, B. C. Sales, D. K. Christen, and D. Mandrus, Two-band superconductivity in LaFeAsO_{0.89}F_{0.11} at very high magnetic fields, *Nature (London)* **453**, 903 (2008).
- [6] G. R. Stewart, Superconductivity in iron compounds, *Rev. Mod. Phys.* **83**, 1589 (2011).
- [7] I. I. Mazin, D. J. Singh, M. D. Johannes, and M. H. Du, Unconventional Superconductivity with a Sign Reversal in the Order Parameter of LaFeAsO_{1-x}F_x, *Phys. Rev. Lett.* **101**, 057003 (2008).
- [8] T. Hanaguri, S. Niitaka, K. Kuroki, and H. Takagi, Unconventional s-wave superconductivity in Fe(Se, Te), *Science* **328**, 474 (2010).
- [9] L. U. L. Shen, N. M. Senozan, and N. E. Phillips, Evidence for Two Energy Gaps in High-Purity Superconducting Nb, Ta, and V, *Phys. Rev. Lett.* **14**, 1025 (1965).
- [10] E. Boaknin, M. A. Tanatar, J. Paglione, D. Hawthorn, F. Ronning, R. W. Hill, M. Sutherland, L. Taillefer, J. Sonier, S. M. Hayden, and J. W. Brill, Heat Conduction in the Vortex State of NbSe₂: Evidence for Multiband Superconductivity, *Phys. Rev. Lett.* **90**, 117003 (2003).
- [11] G. R. Stewart, Non-Fermi-liquid behavior of *d*- and *f*-electron metals, *Rev. Mod. Phys.* **73**, 797 (2001).
- [12] M. Jourdan, A. Zakharov, M. Foerster, and H. Adrian, Evidence for Multiband Superconductivity in the Heavy Fermion Compound UNi₂Al₃, *Phys. Rev. Lett.* **93**, 097001 (2004).
- [13] P. M. C. Rourke, M. A. Tanatar, C. S. Turel, J. Berdeklis, C. Petrovic, and J. Y. T. Wei, Spectroscopic Evidence for Multiple Order Parameter Components in the Heavy Fermion Superconductor CeCoIn₅, *Phys. Rev. Lett.* **94**, 107005 (2005).
- [14] G. Seyfarth, J. P. Brison, M.-A. Méasson, J. Flouquet, K. Izawa, Y. Matsuda, H. Sugawara, and H. Sato, Multiband Superconductivity in the Heavy Fermion Compound PrOs₄Sb₁₂, *Phys. Rev. Lett.* **95**, 107004 (2005).
- [15] R. W. Hill, S. Li, M. B. Maple, and L. Taillefer, Multiband Order Parameters for the PrOs₄Sb₁₂ and PrRu₄Sb₁₂ Skutterudite Superconductors from Thermal Conductivity Measurements, *Phys. Rev. Lett.* **101**, 237005 (2008).
- [16] B. Bergk, V. Petzold, H. Rosner, S.-L. Drechsler, M. Bartkowiak, O. Ignatchik, A. D. Bianchi, I. Sheikin, P. C. Canfield, and J. Wosnitza, Anisotropic Multiband Many-Body Interactions in LuNi₂B₂C, *Phys. Rev. Lett.* **100**, 257004 (2008).
- [17] S. Kuroiwa, Y. Saura, J. Akimitsu, M. Hiraishi, M. Miyazaki, K. H. Satho, S. Takeshita, R. Kadono, Multigap Superconductivity in Sesquicarbides La₂C₃ and Y₂C₃, *Phys. Rev. Lett.* **100**, 097002 (2008).
- [18] A. P. Petrović, R. Lortz, G. Santi, C. Berthod, C. Dubois, M. Decroux, A. Demuer, A. B. Antunes, A. Paré, D. Salloum, P. Gougeon, M. Potel, and O. Fischer, Multiband Superconductivity in the Chevrel Phases SnMo₆S₈ and PbMo₆S₈, *Phys. Rev. Lett.* **106**, 017003 (2011).
- [19] S. Deng, L. Viola, and G. Ortiz, Majorana Modes in Time-Reversal Invariant *s*-Wave Topological Superconductors, *Phys. Rev. Lett.* **108**, 036803 (2012).
- [20] S. Deng, G. Ortiz, and L. Viola, Multiband *s*-wave topological superconductors: Role of dimensionality and magnetic field response, *Phys. Rev. B* **87**, 205414 (2013).
- [21] H. Suhl, B. T. Matthias, and L. R. Walker, Bardeen-Cooper-Schrieffer Theory of Superconductivity in the Case of Overlapping Bands, *Phys. Rev. Lett.* **3**, 552 (1959).
- [22] M. E. Zhitomirsky and V.-H. Dao, Ginzburg-Landau theory of vortices in a multigap superconductor, *Phys. Rev. B* **69**, 054508 (2004).
- [23] A. Chaves, L. Komendová, M. V. Milošević, J. S. Andrade, Jr., G. A. Farias, and F. M. Peeters, Conditions for nonmonotonic vortex interaction in two-band superconductors, *Phys. Rev. B* **83**, 214523 (2011).
- [24] L. Komendová, Y. Chen, A. A. Shanenko, Milošević, and F. M. Peeters, Two-band superconductors: Hidden Criticality Deep in the Superconducting State, *Phys. Rev. Lett.* **108**, 207002 (2012).
- [25] E. Babaev, J. Carlström, and M. Speight, Type-1.5 Superconducting State from an Intrinsic Proximity Effect in Two-Band Superconductors, *Phys. Rev. Lett.* **105**, 067003 (2010).
- [26] J. Carlström, E. Babaev, and M. Speight, Type-1.5 superconductivity in multiband systems: Effects of interband couplings, *Phys. Rev. B* **83**, 174509 (2011).

- [27] Y. Noat, T. Cren, P. Toulemonde, A. San Miguel, F. Debontridder, V. Dubost and D. Roditchev, Two energy gaps in the tunneling-conductance spectra of the superconducting clathrate $\text{Ba}_8\text{Si}_{46}$, *Phys. Rev. B* **81**, 104522 (2010).
- [28] Y. Noat, T. Cren, F. Debontridder, D. Roditchev, W. Sacks, P. Toulemonde and A. San Miguel, Signatures of multigap superconductivity in tunneling spectroscopy, *Phys. Rev. B* **82**, 014531 (2010).
- [29] Y. Noat, T. Cren, V. Dubost, S. Lange, F. Debontridder, P. Toulemonde, J. Marcus, A. Sulpice, W. Sacks and D. Roditchev, Disorder effects in pnictides: a tunneling spectroscopy study, *J. Phys.: Condens. Matter* **22**, 465701 (2010).
- [30] H. Schmidt, J. F. Zasadzinski, K. E. Gray, and D. G. Hinks, Break-junction tunneling on MgB_2 , *Physica C* **385**, 221 (2003).
- [31] D. Mou, R. Jiang, V. Taufour, S. L. Bud'ko, P. C. Canfield, and A. Kaminski, Momentum dependence of the superconducting gap and in-gap states in MgB_2 multi-band superconductor, [arXiv:1504.06347](https://arxiv.org/abs/1504.06347).
- [32] W. L. McMillan, Tunneling model of the superconducting proximity effect, *Phys. Rev.* **175**, 537 (1968).
- [33] N. Schopohl and K. Scharnberg, Tunneling density of states for the two-band model of superconductivity, *Solid State Commun.* **22**, 371 (1977).
- [34] G. M. Japiassú, M. A. Continentino, and A. Troper, Mean-field treatment of the hybridization influence on narrow-band superconductivity, *Phys. Rev. B* **45**, 2986 (1992).
- [35] A. Moreo, M. Daghofer, A. Nicholson, and E. Dagotto, Interband pairing in multiorbital systems, *Phys. Rev. B* **80**, 104507 (2009).
- [36] V. Cvetkovic and O. Vafek, Space group symmetry, spin-orbit coupling, and the low-energy effective Hamiltonian for iron-based superconductors, *Phys. Rev. B* **88**, 134510 (2013).
- [37] T. T. Ong and P. Coleman, Tetrahedral and Orbital Pairing: A Fully Gapped Scenario for the Iron-Based Superconductors, *Phys. Rev. Lett.* **111**, 217003 (2013).
- [38] A. Hinojosa and A. V. Chubukov, Gap structure in Fe-based superconductors with accidental nodes: The role of hybridization, *Phys. Rev. B* **91**, 224502 (2015).
- [39] W. V. Liu and F. Wilczek, Interior Gap Superfluidity, *Phys. Rev. Lett.* **90**, 047002 (2003).
- [40] E. Gubankova, W. V. Liu and F. Wilczek, Breached Pairing Superfluidity: Possible Realization in QCD, *Phys. Rev. Lett.* **91**, 032001 (2003).
- [41] A. M. Black-Schaffer and A. V. Balatsky, Odd-frequency superconducting pairing in multiband superconductors, *Phys. Rev. B* **88**, 104514 (2013).
- [42] V. L. Berezinskii, New model of the anisotropic phase of superfluid He^3 , *JETP Lett.* **20**, 287 (1974) [*Zh. Eksp. Teor. Fiz.* **20**, 628 (1974)].
- [43] A. Balatsky and E. Abrahams, New class of singlet superconductors which break the time reversal and parity, *Phys. Rev. B* **45**, 13125(R) (1992).
- [44] E. Abrahams, A. Balatsky, D. J. Scalapino, and J. R. Schrieffer, Properties of odd-gap superconductors, *Phys. Rev. B* **52**, 1271 (1995).
- [45] F. S. Bergeret, A. F. Volkov, and K. B. Efetov, Long-Range Proximity Effects in Superconductor-Ferromagnet Structures, *Phys. Rev. Lett.* **86**, 4096 (2001).
- [46] F. S. Bergeret, A. F. Volkov, and K. B. Efetov, Odd triplet superconductivity and related phenomena in superconductor-ferromagnet structures, *Rev. Mod. Phys.* **77**, 1321 (2005).
- [47] Y. Tanaka and A. A. Golubov, Theory of the Proximity Effect in Junctions with Unconventional Superconductors, *Phys. Rev. Lett.* **98**, 037003 (2007).
- [48] Y. Tanaka, A. A. Golubov, S. Kashiwaya, and M. Ueda, Anomalous Josephson Effect Between Even- and Odd-Frequency Superconductors, *Phys. Rev. Lett.* **99**, 037005 (2007).
- [49] Y. Tanaka, Y. Tanuma, and A. A. Golubov, Odd-frequency pairing in normal-metal/superconductor junctions, *Phys. Rev. B* **76**, 054522 (2007).
- [50] A. Aperis, P. Maldonado, and P. M. Oppeneer, *Ab initio* theory of magnetic-field-induced odd-frequency two-band superconductivity in MgB_2 , *Phys. Rev. B* **92**, 054516 (2015).
- [51] F. Parhizgar and A. M. Black-Schaffer, Unconventional proximity-induced superconductivity in bilayer systems, *Phys. Rev. B* **90**, 184517 (2014).
- [52] See, e.g., G. D. Mahan, *Many-Particle Physics* (Plenum Publishers, New York, 2000).
- [53] P. Coleman, E. Miranda, and A. Tsvelik, Possible Realization of Odd-Frequency Pairing in Heavy Fermion Compounds, *Phys. Rev. Lett.* **70**, 2960 (1993).
- [54] A. M. Black-Schaffer and A. V. Balatsky, Odd-frequency superconducting pairing in topological insulators, *Phys. Rev. B* **86**, 144506 (2012).
- [55] L.-F. Zhang, L. Covaci, and F. M. Peeters, Tomasch effect in nanoscale superconductors, *Phys. Rev. B* **91**, 024508 (2015).
- [56] T. Yokoyama, Y. Tanaka, and A. A. Golubov, Manifestation of the odd-frequency spin-triplet pairing state in diffusive ferromagnet/superconductor junctions, *Phys. Rev. B* **75**, 134510 (2007).
- [57] H. P. Dahal, E. Abrahams, D. Mozyrsky, Y. Tanaka, and A. V. Balatsky, Wave function for odd-frequency superconductors, *New J. Phys.* **11**, 065005 (2009).
- [58] Y. Asano and Y. Tanaka, Majorana fermions and odd-frequency Cooper pairs in a normal-metal nanowire proximity-coupled to a topological superconductor, *Phys. Rev. B* **87**, 104513 (2013).
- [59] Y. Tanaka, M. Sato, and N. Nagaosa, Symmetry and topology in superconductors - odd-frequency pairing and edge states, *J. Phys. Soc. Jpn.* **81**, 011013 (2012).
- [60] A. M. Black-Schaffer and A. V. Balatsky, Proximity-induced unconventional superconductivity in topological insulators, *Phys. Rev. B* **87**, 220506(R) (2013).
- [61] J. Linder and J. W. A. Robinson, Anomalous odd-frequency pairing correlations in Zeeman-split superconductors, [arXiv:1409.3228](https://arxiv.org/abs/1409.3228).